energy&fuels

Article

pubs.acs.org/EF

Direct Analysis of Thin-Layer Chromatography Separations of Petroleum Samples by Laser Desorption Ionization Fourier Transform Ion Cyclotron Resonance Mass Spectrometry Imaging

Donald F. Smith,[†,‡] Amy M. McKenna,[‡] Yuri E. Corilo,[‡,§] Ryan P. Rodgers,[‡,§,∥] Alan G. Marshall,[‡,∥] and Ron M. A. Heeren*[,†]

[†]FOM Institute AMOLF, Science Park 104, 1098 XG Amsterdam, Netherlands

[‡]National High Magnetic Field Laboratory, and [§]Future Fuels Institute, Florida State University, 1800 East Paul Dirac Drive, Tallahassee Florida 32310-4005, United States

[∥]Department of Chemistry and Biochemistry, Florida State University, 95 Chieftain Way, Tallahassee, Florida 32303, United States

ABSTRACT: We present an analytical method for direct analysis of thin-layer chromatography (TLC) separations of petroleum samples by laser desorption ionization (LDI) coupled to Fourier transform ion cyclotron resonance mass spectrometry (FT-ICR MS) imaging. LDI of TLC plates selectively ionizes condensed aromatic hydrocarbons and facilitates two-dimensional imaging of TLC-separated petroleum compounds. Molecular-level characterization available only with ultrahigh-resolution FT-ICR MS provides elemental composition assignment and surpasses conventional TLC readout-based flame ionization detection. Resolution and assignment of migrated molecules targeted by LDI combined with FT-ICR MS provides elemental composition assignment and, therefore, chemical information, i.e., heteroatom class, aromaticity (double bond equivalents), and carbon number. Here, three petroleum samples (a field deposit, a crude oil, and a tar ball) were TLC-separated by their solubility in *n*-heptane and imaged by LDI FT-ICR MS.

INTRODUCTION

Thin-layer chromatography (TLC) is a convenient, rapid, and simple technique for petroleum characterization. It is commonly used for hydrocarbon-type analysis, for example, to determine saturates, aromatics, resins, and asphaltenes (SARA) fractions. TLC is typically coupled with flame ionization detection (TLC−FID), where the response varies linearly with sample quantity and hydrocarbon signal response is directly proportional to the number of carbons.[12] However, FID signal response varies with heteroatom-containing compounds (e.g., nitrogen, oxygen, and sulfur), and quantitation is problematic.[3] Element-specific detectors, such as flame photometric detection for sulfur/phosphorus,[4] flame thermionic ionization detection for nitrogen/halogens,[5] and chemiluminescent detection for nitrogen,[6] improve element specificity for TLC−FID analysis. Although TLC−FID can be used for quantitative determination of chromatographic yields, little molecular-level information can be gained.

Most petroleum TLC−FID studies are commonly performed with an Iatroscan instrument with chromatography rods (Iatron Laboratories, Tokyo, Japan) rather than plates. However, plate-based TLC coupled with mass spectrometry (MS) provides a high sensitivity readout with chemical and structural information when combined with tandem mass spectrometry.[7−9] These methods are often coupled with laser desorption ionization (LDI) or matrix-assisted laser desorption ionization (MALDI). An identical separation mechanism is maintained from chromatography rod to plate, but TLC plates can be directly analyzed to create a second mass spectral dimension for the TLC chromatogram, thereby enabling quick chemical readout of new chromatography methods, with easy implementation for existing (MA)LDI-equipped mass spectrometers.

TLC separation of petroleum samples with mass spectrometric readout could provide local characterization of petroleum samples. Chirinos et al. coupled TLC separation to laser-ablation inductively coupled plasma MS with a modified SARA TLC plate separation and targeted the asphaltene fraction to determine vanadium/nickel proportionality.[10] A series of line scans across the asphaltene spot were collected to create a "raster line ablation pattern" image of vanadium in the spot. However, no further analysis was performed for the remainder of the chromatogram, likely because of a lack of elemental information on interest in the other separated fractions.

Recently, atmospheric pressure laser ionization (APLI; 248 nm laser wavelength) and LDI (355 nm laser wavelength) coupled to Fourier transform ion cyclotron resonance mass spectrometry (FT-ICR MS) has provided detailed molecular analysis of crude oils,[11,12] shale oils,[13] heavy fuel oil,[14] and asphaltenes[15] as well as coupling with online liquid chromatography.[16] Ultrahigh mass resolving power and sub-part-per-million (ppm) mass measurement accuracy available only with FT-ICR MS[17] resolve and assign the tens of thousands of compounds in complex petroleum samples.[18−21] LDI and APLI ionize petrocompounds, such as condensed aromatic hydrocarbons and nitrogen-, oxygen-, and sulfur-containing compounds. The detailed chemical speciation by

Received: June 28, 2014
Revised: August 19, 2014
Published: September 11, 2014

dx.doi.org/10.1021/ef501439w | *Energy Fuels* 2014, 28, 6284−6288

FT-ICR MS combined with targeted imaging by LDI of TLC chromatograms provides a unique tool for molecular-level imaging of environmental petroleum samples.

Here, we present a direct chemical readout of TLC chromatograms by LDI FT-ICR MS imaging. Three petroleum samples, representing a range of origin, complexity, and composition, were chosen to test the methodology. Thousands of species were detected, and elemental formulas could be assigned to map the chemical properties of the separated fractions across the TLC chromatogram.

EXPERIMENTAL SECTION

Samples and Reagents. High-performance liquid chromatography (HPLC)-grade *n*-heptane and dichloromethane were purchased from Sigma-Aldrich (Zwijndrecht, Netherlands) and analytical research-grade isopropanol was purchased from Biosolve (Valkenswaard, Netherlands). Three petroleum samples of different origin were selected: field deposit from an offshore crude oil production facility,[22] Deepwater Horizon light crude oil,[23] and a tar ball collected off the coast of Louisiana in 2011. All samples were diluted in dichloromethane: field deposit, 400 mg/mL; light crude oil, 200 mg/mL; and tar ball, 100 mg/mL.

TLC. Samples were micropipetted 7 mm from the bottom of an aluminum-backed silica gel TLC foil (Sigma-Aldrich, St. Louis, MO). Samples were deposited in 2 μL aliquots to yield 800 μg of field deposit, 200 μg of light crude oil, and 100 μg of tar ball. The mobile phase consisted of 95:5 (vol/vol) *n*-heptane/isopropanol to separate compounds based on their solubility in *n*-heptane and polarity, as previously reported.[10] Plate TLC has a distinct advantage when *n*-heptane is used as the mobile phase, because asphaltenes will precipitate. In a traditional capillary column, precipitation could cause the column to clog and block other components; however, for the TLC plate used here, the other components are free to migrate around the asphaltenes that have precipitated at the origin. The development chamber was equilibrated for 5 min and developed for approximately 4 min, air-dried, and visualized in a Spectroline CM-10 fluorescence analysis cabinet with an ultraviolet lamp (254 nm, Spectroline ENF-260/F, Spectronics Corporation, Westbury, NY).

FT-ICR MS Imaging. Dry TLC foil attached to a stainless-steel MALDI target with double-sided conductive tape was analyzed without matrix with a custom-built 9.4 T FT-ICR mass spectrometer for MS imaging.[24] A Nd:YAG laser (355 nm, Wedge model 255, Bright-Solutions, Cura Carpignano, Italy) was used for laser desorption directly from the TLC foil, with 500 laser shots per position at 1 kHz repetition rate. A spectral stitching strategy was employed to reduce ion number-related effects in the ICR cell and maintain high mass resolving power.[25] Four mass spectra were collected at each pixel position by stepping a mass-selective quadrupole from m/z 250 to 610 at a window width of 90 Da. The $X-Y$ translational stage was automatically offset by 300 μm for each spectrum, resulting in a square pattern for each pixel, as shown in Figure 1. A free-form region of interest was used to highlight the three TLC separations, with a stage raster step size of 1 mm.

Laser-desorbed ions were collected by a radio-frequency-only hexapole ion guide and accumulated in an external octopole trap before transfer to the ICR cell, in which the ions were cooled with a pulse of argon before broadband frequency chirp excitation and broadband detection (2 Mword time-domain transient; 1.57 s, Fourier-limited mass resolving power; $m/\Delta m_{50\%}$ = 283 000 at m/z 400, in which $\Delta m_{50\%}$ is the magnitude-mode spectral peak width at half-maximum peak height). The ICR cell was a seven-segment electrically compensated cylindrical cell based on the design by Tolmachev et al.,[26] with 120° detection electrodes and 60° excitation electrodes, as described by Kaiser et al.[27] Instrument control was provided by the AMOLF-developed work-flow-based arbitrary waveform generator (AWG) software.[28,29]

Data Processing. The AMOLF-developed Chameleon software was used for data processing. Each mass spectrum was internally calibrated with respect to high abundance hydrocarbon homologous series; different homologous series were used for each quadrupole mass slice. Mass spectra were inserted into a high mass resolution "Mosaic Datacube"[30,31] and peak-picked above a signal-to-noise ratio (S/N) of 5. Peaklists were analyzed with custom-developed Matlab code [MATLAB, version 7.13.0.564 (64 bit), MathWorks, Natick, MA] for root-mean-square (rms) mass measurement error calculations and automatic image generation.[30] Elemental compositions were assigned to peaks with a magnitude greater than 6 times the standard deviation of the noise (6σ), and isoabundance-contoured double bond equivalents (DBE = number of rings plus double bonds to carbon) versus carbon number plots were produced by PetroOrg data processing software.[32]

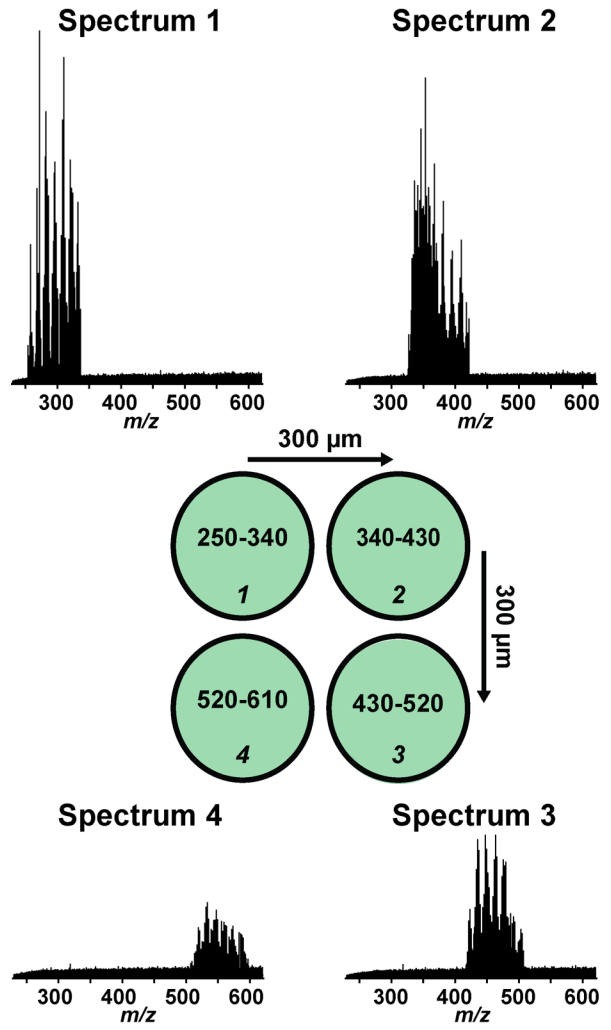

Figure 1. Mass spectral segment stitching strategy. A mass-selective quadrupole was used to select four mass segments (each 90 Da in width), and the $X-Y$ translational stage was offset by 300 μm to collect each spectrum from a fresh sample position. The "stitched" mass spectrum thus represents ~4× as many ions as would have been present for a single broadband mass spectrum.

RESULTS AND DISCUSSION

Mass Spectral Segment Stitching. Multiple time-domain acquisitions are typically collected and co-added for FT-ICR MS analysis of complex mixtures to increase the S/N and dynamic range and minimize space-charge effects in the ICR cell.[18,33] However, signal averaging is not possible for surface analyses, such as TLC plate imaging, because of the finite spatial extent of surface samples. Therefore, a spectral stitching

dx.doi.org/10.1021/ef501439w | Energy Fuels 2014, 28, 6284−6288

approach was selected to maintain high mass resolving power and S/N across the target mass range (m/z 250−610). This mass range was chosen to sample the center of the molecular weight distribution expected for analysis of petroleum samples by LDI FT-ICR MS, as determined by Cho et al.[12,13]

Figure 2 shows average mass spectra (peak picked) for the three samples analyzed by LDI FT-ICR MS imaging. The mass

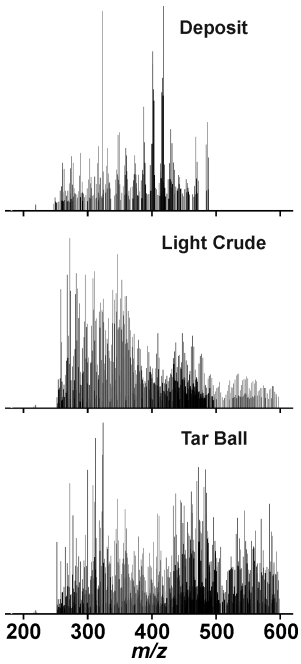

Figure 2. Average mass spectra (peak picked) from LDI FT-ICR MS imaging of a TLC separation. (Top) Deposit. (Middle) Light crude oil. (Bottom) Tar ball. The mass cutoff from quadrupole isolation is clearly visible at m/z 250 and 600, and slight edge effects result from partial overlap between the selected m/z ranges (i.e., m/z range from 520 to 250 = 270, spanned by four m/z 90 segments = 360).

distributions from selected quadrupole isolation windows agree with previous LDI analyses of crude oil.[12,13] However, here, ions in the range of m/z 250−610 were targeted; thus, lower abundance species at low and high m/z are not detected in our measurements. Further, edge effects are observed as areas of lower abundance, where the selected m/z ranges have partial overlap. The spectral distribution for each petroleum sample is unique, as expected, for distinct samples. The deposit shows a distinct distribution centered near m/z 400 (Figure 2a), whereas the light crude oil (Figure 2b) and the weathered tar ball (Figure 2c) show broader mass distributions, with the tar ball containing more compounds above m/z 500. The average molecular weight distribution by LDI from the deposit matches previous reports by atmospheric pressure photoionization (APPI) reported by Juyal et al.[22] and indicates comparable molecular weight distributions by spectral stitching from TLC measurements.

TLC Fractionation. The fractionation used here is similar to a SARA fractionation, but here, molecules are eluted isocratically with a nonpolar mobile phase (*n*-heptane) to separate compounds by polarity; the least polar molecules migrate the farthest (saturates), followed by more polar molecules (e.g., aromatics and resins). The most polar species, the asphaltenes, are non-mobile and precipitate at the origin.[34,35] Figure 3 shows total ion count (TIC) for all mass spectral peaks in each pixel

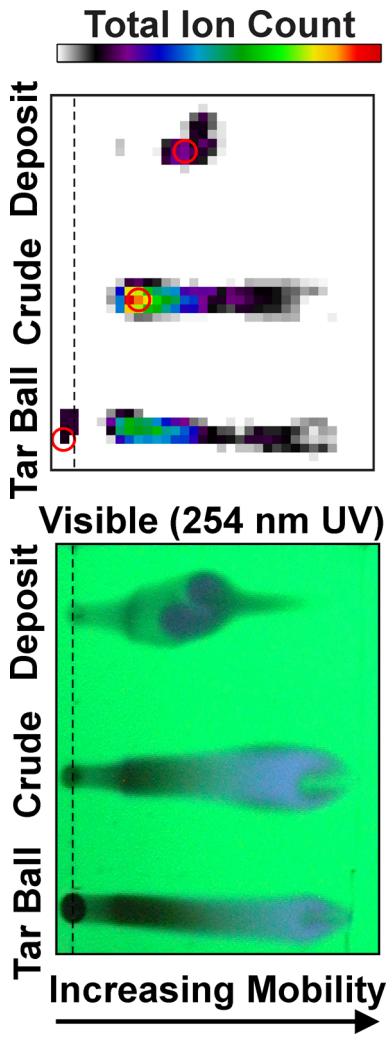

Figure 3. Images of TLC separations for a petroleum deposit, light crude oil, and tar ball. (Top) Total ion count from LDI FT-ICR MS. (Bottom) Visible fluorescence (254 nm UV light). The dotted line indicates the chromatographic origin. Isoabundance-contoured plots of DBE versus carbon number for the hydrocarbon class of the pixels circled in red are shown in Figure 4.

(top) and a fluorescence image of the developed TLC plate (bottom; 254 nm UV illumination). The TIC image reproduces spatial features of the TLC plate development, such as the area of high ion abundance at the center of the deposit separation (aromatic fraction) and the tar ball asphaltene fraction that does not move from the origin. The structure observed for the deposit separation is likely due to two sample aliquots that were spotted at the origin before separation. No asphaltenes were detected for the light crude oil or the field deposit, in agreement with previous reports.[22,23,36] For all samples, the TIC signal decreases for the saturate fraction, because less aromatic molecules in the saturate fraction do not absorb the 355 nm laser light as well and, thus, are less efficiently desorbed and ionized.

Compositional Comparisons. Each pixel in Figure 3 yields a mass spectrum in which elemental compositions can be assigned to measured masses to determine type and number of heteroatoms (N, O, and S) and degree of aromaticity (DBE).[37] Isoabundance-contoured plots of DBE versus carbon number for each heteroatom class facilitate rapid visualization of compositional differences between molecules of the same

dx.doi.org/10.1021/ef501439w | *Energy Fuels* 2014, 28, 6284−6288

class for different samples. The hydrocarbon class (HC; molecules containing only carbon and hydrogen) has the highest relative abundance for all three samples. Figure 4 shows

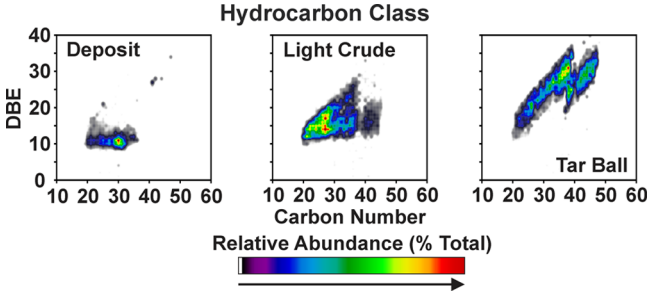

Figure 4. Isoabundance-contoured plots of DBE versus carbon number for members of the hydrocarbon class from the pixels circled in red in Figure 3. (Left) Deposit aromatics. (Middle) Light crude oil resins. (Right) Tar ball asphaltenes.

the HC class derived from highlighted pixels circled in red in Figure 3. The field deposit shows a high relative abundance of hydrocarbons of DBE 10 and 11 (left panel of Figure 4). The hydrocarbons from the light crude oil that elute slightly off-origin (middle panel of Figure 4), in the resin fraction, span a broad compositional space, with elemental compositions that correspond to condensed aromatic compounds that approach the planar aromatic limit.[38,39] The compositional gap observed in the top right of the light crude plot is believed to be the separation of asphaltenic and maltenic species on the TLC plate.[40] Non-mobile compounds from the tar ball (right panel of Figure 4) correspond to highly aromatic HC species, again concentrated near the polycyclic aromatic hydrocarbon limit.

Compositional data from molecular formula assignments can be used to track molecular changes along the chromatographic axis. Figure 5 shows weighted average carbon number and DBE versus the pixel number (along the chromatographic axis) for the light crude oil (top panel of Figure 5) and the tar ball (bottom panel of Figure 5). The average DBE for the light crude oil is similar for the three resin positions but increases in the aromatic fractions and decreases slightly in the saturate fraction. The average carbon number is low in the first resin fraction, increases and remains constant across the other resin and aromatic fractions, and decreases in the saturate fraction. For the tar ball, the asphaltene fraction has the highest average DBE and carbon number. Upon elution, both average DBE and carbon number follow similar trends: a decrease is seen in the resin fraction, followed by a slight increase in the aromatic fraction, and again a decrease for the saturate fraction.

FUTURE PROSPECTS

Here, we present a method for detailed chemical speciation of TLC separations by FT-ICR MS imaging with LDI. Although the present separation is quite simple, the method could easily be extended to more complex TLC separations. Adaptation of most established TLC–FID separation methods should be possible, with the benefit of increased chemical speciation. Multiple elution solvents could be employed, and orthogonal separations could easily be accomplished by simply turning the TLC plate by 90° and eluting in a different plane. Further, the use of different TLC stationary matrices offers additional separation possibilities. The 355 nm laser light used here is effective for desorption/ionization of condensed aromatic

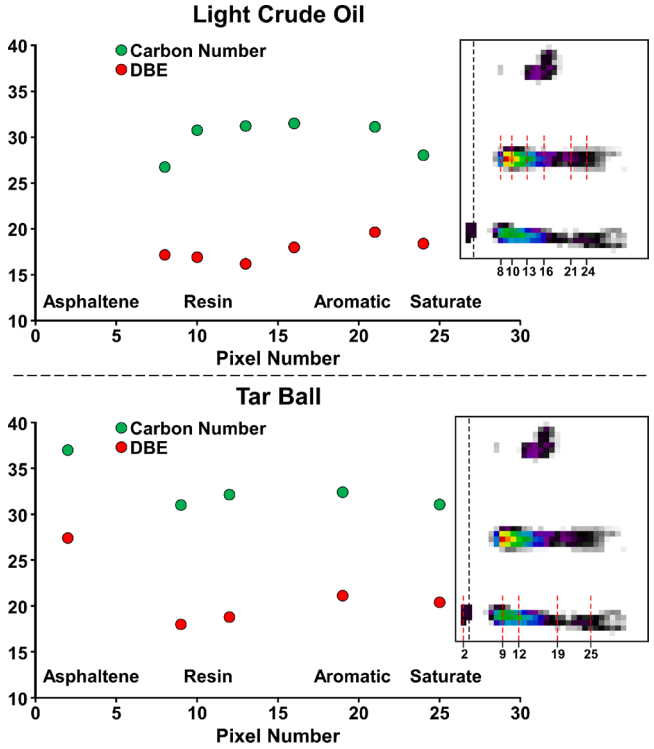

Figure 5. Weighted average carbon number (green) and DBE (red) versus pixel position along the chromatographic axis for the hydrocarbon class. (Top) Light crude oil. (Bottom) Tar ball.

species, without the need for additional matrix application. However, an UV-absorbing matrix might provide enhanced desorption/ionization of less aromatic species and more polar heteroatom-containing species. Moreover, the addition of silver ions could enhance the ionization and detection of long-chain saturated molecules.[41,42] Negative-ion detection can yield additional information about the chemical composition of oxygen species, in particular, naphthenic acids. Together, the combination of TLC with FT-ICR MS imaging presents a simple and robust method for detailed chemical speciation of TLC separations.

AUTHOR INFORMATION

Corresponding Author

*Telephone: +31-20-754-7100. Fax: +31-20-754-7290. E-mail: r.heeren@amolf.nl.

Notes

The authors declare no competing financial interest.

ACKNOWLEDGMENTS

This work is part of the research program of the Foundation for Fundamental Research on Matter (FOM), which is part of the Netherlands Organization for Scientific Research (NWO). This publication was supported by the Dutch national program COMMIT. Work was supported by the National Science Foundation (NSF) Division of Materials Research through DMR-11-57490, the NSF Division of Chemistry (through CHE-1019193), the Florida State University Future Fuels Institute, the BP/The Gulf of Mexico Research Initiative to the Deep-C Consortium, and the State of Florida.

REFERENCES

(1) Karlsen, D. A.; Larter, S. R. *Org. Geochem.* **1991**, *17*, 603–617.

(2) Holm, T. *J. Chromatogr. A* **1999**, *842*, 221−227.
(3) Jiang, C. Q.; Larter, S. R.; Noke, K. J.; Snowdon, L. R. *Org. Geochem.* **2008**, *39*, 1210−1214.
(4) Ogasawara, M.; Tsuruta, K.; Arao, S. *J. Chromatogr. A* **2002**, *973*, 151−158.
(5) Patterson, P. L. *Lipids* **1985**, *20*, 503−509.
(6) Holmesa, S. A. *J. Chromatogr. A* **1989**, *465*, 345−358.
(7) Fuchs, B.; Suss, R.; Nimptsch, A.; Schiller, J. *Chromatographia* **2009**, *69*, S95−S105.
(8) Cheng, S. C.; Huang, M. Z.; Shiea, J. *J. Chromatogr. A* **2011**, *1218*, 2700−2711.
(9) Gusev, A. I. *Fresenius' J. Anal. Chem.* **2000**, *366*, 691−700.
(10) Chirinos, J.; Oropeza, D.; González, J.; Ranaudo, M.; Russo, R. E. *Energy Fuels* **2013**, *27*, 2431−2436.
(11) Schrader, W.; Panda, S. K.; Brockmann, K. J.; Benter, T. *Analyst* **2008**, *133*, 867−869.
(12) Cho, Y.; Witt, M.; Kim, Y. H.; Kim, S. *Anal. Chem.* **2012**, *84*, 8587−8594.
(13) Cho, Y.; Jin, J. M.; Witt, M.; Birdwell, J. E.; Na, J.-G.; Roh, N.-S.; Kim, S. *Energy Fuels* **2012**, *27*, 1830−1837.
(14) Schmitt-Kopplin, P.; Englmann, M.; Rossello-Mora, R.; Schiewek, R.; Brockmann, K. J.; Benter, T.; Schmitz, O. J. *Anal. Bioanal. Chem.* **2008**, *391*, 2803−2809.
(15) Gaspar, A.; Zellermann, E.; Lababidi, S.; Reece, J.; Schrader, W. *Anal. Chem.* **2012**, *84*, 5257−5267.
(16) Lababidi, S.; Panda, S. K.; Andersson, J. T.; Schrader, W. *Anal. Chem.* **2013**, *85*, 9478−9485.
(17) Marshall, A. G.; Hendrickson, C. L.; Jackson, G. S. *Mass Spectrom. Rev.* **1998**, *17*, 1−35.
(18) Marshall, A. G.; Rodgers, R. P. *Acc. Chem. Res.* **2004**, *37*, 53−59.
(19) Rodgers, R. P.; Schaub, T. M.; Marshall, A. G. *Anal. Chem.* **2005**, *77*, 20A−27A.
(20) Marshall, A. G.; Rodgers, R. P. *Proc. Natl. Acad. Sci. U. S. A.* **2008**, *105*, 18090−18095.
(21) Hsu, C. S.; Hendrickson, C. L.; Rodgers, R. P.; McKenna, A. M.; Marshall, A. G. *J. Mass Spectrom.* **2011**, *46*, 337−343.
(22) Juyal, P.; McKenna, A. M.; Yen, A.; Rodgers, R. P.; Reddy, C. M.; Nelson, R. K.; Andrews, A. B.; Atolia, E.; Allenson, S. J.; Mullins, O. C.; Marshall, A. G. *Energy Fuels* **2010**, *25*, 172−182.
(23) McKenna, A. M.; Nelson, R. K.; Reddy, C. M.; Savory, J. J.; Kaiser, N. K.; Fitzsimmons, J. E.; Marshall, A. G.; Rodgers, R. P. *Environ. Sci. Technol.* **2013**, *47*, 7530−7539.
(24) Smith, D. F.; Aizikov, K.; Duursma, M. C.; Giskes, F.; Spaanderman, D.-J.; McDonnell, L. A.; O'Connor, P. B.; Heeren, R. M. A. *J. Am. Soc. Mass. Spectrom.* **2011**, *22*, 130−137.
(25) Gaspar, A.; Schrader, W. *Rapid Commun. Mass Spectrom.* **2012**, *26*, 1047−1052.
(26) Tolmachev, A. V.; Robinson, E. W.; Wu, S.; Kang, H.; Lourette, N. M.; Pasa-Tolic, L.; Smith, R. D. *J. Am. Soc. Mass. Spectrom.* **2008**, *19*, 586−597.
(27) Kaiser, N. K.; Savory, J. J.; McKenna, A. M.; Quinn, J. P.; Hendrickson, C. L.; Marshall, A. G. *Anal. Chem.* **2011**, *83*, 6907−6910.
(28) Mize, T. H.; Taban, I.; Duursma, M.; Seynen, M.; Konijnenburg, M.; Vijftigschild, A.; Doornik, C. V.; Rooij, G. V.; Heeren, R. M. A. *Int. J. Mass Spectrom.* **2004**, *235*, 243−253.
(29) Taban, L. M.; van der Burgt, Y. E. M.; Duursma, M.; Takats, Z.; Seynen, M.; Konijnenburg, M.; Vijftigschild, A.; Attema, I.; Heeren, R. M. A. *Rapid Commun. Mass Spectrom.* **2008**, *22*, 1245−1256.
(30) Smith, D. F.; Kharchenko, A.; Konijnenburg, M.; Klinkert, I.; Pasa-Tolic, L.; Heeren, R. M. A. *J. Am. Soc. Mass. Spectrom.* **2012**, *23*, 1865−1872.
(31) Klinkert, I.; Chughtai, K.; Ellis, S. R.; Heeren, R. M. A. *Int. J. Mass Spectrom.* **2013**, *362*, 40−47.
(32) *PetroOrg Software*; Florida State University, Tallahassee, FL; http://software.petroorg.com.
(33) Jeffries, J. B.; Barlow, S. E.; Dunn, G. H. *Int. J. Mass Spectrom. Ion Processes* **1983**, *54*, 169−187.
(34) Jewell, D. M.; Weber, J. H.; Bunger, J. W.; Plancher, H.; Latham, D. R. *Anal. Chem.* **1972**, *44*, 1391−1395.
(35) ASTM International. *ASTM D2007-93. Standard Test Method for Characteristic Groups in Rubber Extender and Processing Oils by the Clay-Gel Adsorption Chromatographic Method*; ASTM International: West Conshohocken, PA, 1993.
(36) Reddy, C. M.; Arey, J. S.; Seewald, J. S.; Sylva, S. P.; Lemkau, K. L.; Nelson, R. K.; Carmichael, C. A.; McIntyre, C. P.; Fenwick, J.; Ventura, G. T.; Van Mooy, B. A. S.; Camilli, R. *Proc. Natl. Acad. Sci. U. S. A.* **2012**, *109*, 20229−20234.
(37) McLafferty, F. W.; Turecek, F. *Interpretation of Mass Spectra*; University Science Book: Mill Valley, CA, 1993.
(38) Hsu, C. S.; Lobodin, V. V.; Rodgers, R. P.; McKenna, A. M.; Marshall, A. G. *Energy Fuels* **2011**, *25*, 2174−2178.
(39) Lobodin, V. V.; Marshall, A. G.; Hsu, C. S. *Anal. Chem.* **2012**, *84*, 3410−3416.
(40) Podgorski, D. C.; Corilo, Y. E.; Nyadong, L.; Lobodin, V. V.; Bythell, B. J.; Robbins, W. K.; McKenna, A. M.; Marshall, A. G.; Rodgers, R. P. *Energy Fuels* **2012**, *27*, 1268−1276.
(41) Lorente, E.; Berrueco, C.; Herod, A. A.; Millan, M.; Kandiyoti, R. *Rapid Commun. Mass Spectrom.* **2012**, *26*, 1581−1590.
(42) Mennito, A. S.; Qian, K. *Energy Fuels* **2013**, *27*, 7348−7353.